

Spatial heterogeneity of subsurface soil texture drives landscape-scale patterns of woody patches in a subtropical savanna

Yong Zhou  · Thomas W. Boutton  · X. Ben Wu  · Chenghai Yang

Received: 10 November 2016 / Accepted: 11 February 2017 / Published online: 17 February 2017
© Springer Science+Business Media Dordrecht 2017

Abstract

Context In the Rio Grande Plains of southern Texas, subtropical savanna vegetation is characterized by a two-phase pattern consisting of discrete woody patches embedded within a C₄ grassland matrix. Prior trench transect studies have suggested that, on upland portions of the landscape, large woody patches (groves) occur on non-argillic inclusions, while small woody patches (clusters) are dispersed among herbaceous vegetation where the argillic horizon is present. **Objective** To test whether spatial heterogeneity of subsurface soil texture drives the landscape-scale pattern of woody patches in this subtropical savanna. **Methods** Landscape-scale spatial patterns of soil texture were quantified by taking spatially-specific soil samples to a depth of 1.2 m in a 160 m × 100 m plot. Kriged maps of soil texture were developed, and the locations of non-argillic inclusions were mapped.

Results Visual comparison of kriged maps of soil texture to a high resolution aerial photograph of the study area revealed that groves were present exclusively where the non-argillic inclusions were present. This clear visual relationship was further supported by positive correlations between soil sand concentration in the lower soil layers and total fine root biomass which mapped the locations of groves.

Conclusions Subsurface non-argillic inclusions may favor the establishment and persistence of groves by enabling root penetration deeper into the profile, providing greater access to water and nutrients that are less accessible on those portions of the landscape where the argillic horizon is present, thereby regulating the distribution of grove vegetation and structuring the evolution of this landscape.

Keywords Spatial heterogeneity · Subsurface soil texture · Non-argillic inclusions · Argillic horizon · Woody patches · Landscape evolution · Subtropical savanna

Electronic supplementary material The online version of this article (doi:[10.1007/s10980-017-0496-9](https://doi.org/10.1007/s10980-017-0496-9)) contains supplementary material, which is available to authorized users.

Y. Zhou (✉) · T. W. Boutton · X. B. Wu
Department of Ecosystem Science and Management,
Texas A&M University, College Station, TX 77843, USA
e-mail: zhouyong1222@tamu.edu

C. Yang
Aerial Application Technology Research Unit, USDA-ARS, 3103 F and B Road, College Station, TX 77845, USA

Introduction

Savannas are comprised of two divergent growth forms, trees and grasses, and are globally important ecosystems that sustain the livelihoods of a large proportion of the world's human population (Scholes and Archer 1997; Sankaran et al. 2005). In these biomes, patchiness of woody cover is a chief

characteristic and determinant of ecosystem services (Pringle et al. 2010). The abundance and distribution of woody patches has the potential to profoundly influence species diversity (Ratajczak et al. 2012), plant and livestock production (Anadón et al. 2014), as well as many other aspects of ecosystem function, including hydrological and biogeochemical cycles (i.e. “island of fertility”, Schlesinger et al. 1996). Since savannas represent an intermediate/dynamic physiognomy between closed-canopy woodlands and open grasslands, many efforts are underway to assess the factors that determine the relative abundances of woody versus herbaceous components, and to clarify the mechanisms that permit trees and grasses to coexist without the exclusion of one growth form by the other (e.g. Scholes and Archer 1997; Sankaran et al. 2004, 2005; Buitenwerf et al. 2012). However, the mechanisms that regulate the distribution of woody patches in savannas remain uncertain. Because savannas are experiencing increased woody plant abundance globally (Van Auken 2000) and are potentially susceptible to future climate change (Buitenwerf et al. 2012; Volder et al. 2013; Scheiter et al. 2015), an improved understanding of factors that structure the spatial patterns of woody patches in savannas is necessary to better represent this phenomenon in integrated climate-biogeochemical models (Liu et al. 2011), and to improve land management efforts in these regions (Sankaran et al. 2005).

The distribution of woody patches in savannas could be controlled by climate, soils, disturbance regimes (e.g. herbivory and fire), and/or interactions between those factors (Higgins et al. 2000; Zou et al. 2005; Sileshi et al. 2010; Sankaran et al. 2013). Besides climate, which is important at larger scales, subtle spatial heterogeneity in soil properties at the landscape-scale can produce corresponding patchiness in the distribution of woody vegetation in savannas (McAuliffe 1994; Sileshi et al. 2010). This spatial heterogeneity in soils can be a consequence of either pedogenic or biotic processes. For example, in many arid and semiarid savanna ecosystems, termite activities could produce vegetation patterns at different spatial scales by altering soil properties to impart substrate heterogeneity (Arshad 1982; Sileshi et al. 2010; Bonachela et al. 2015). Discontinuity of subsurface soil horizons formed pedogenically is a common feature of soil development in arid and semiarid regions. Spatial heterogeneity of subsurface soil

texture caused by discontinuous soil horizons could affect the abundance and distribution of roots (Watts 1993; Schenk and Jackson 2005) and the movement and availability of soil water and nutrients (McAuliffe 1994; Hamerlynck et al. 2000; Zou et al. 2005), thereby affecting the distribution of woody plants in savannas. For example, coarse-textured subsoils permit root penetration deeper into the soil profile through reduced resistance (Schenk and Jackson 2005) and enable greater infiltration and deeper percolation of water (Brown and Archer 1990), in turn favoring the establishment and persistence of deeply rooted woody plants capable of exploiting soil moisture at greater depths.

In the subtropical Rio Grande Plains of southern Texas, woody plants have markedly increased during the past century (Archer et al. 1988; Boutton et al. 1998; Archer et al. 2001), and upland portions of the landscape display strong patchiness in the distribution of woody vegetation (Archer et al. 1988; Archer 1995). In this region, small discrete woody clusters (generally <100 m² in canopy area) comprised of multiple shrub species organized around a central honey mesquite (*Prosopis glandulosa*) tree, and large groves (generally >100 m²) that coalesced from several clusters are embedded in a C₄ grassland matrix (Archer 1995; Bai et al. 2012). Previous studies in which trenches were excavated along transects from open grassland into the centers of groves showed that subsurface soil horizons were not laterally continuous, with non-argillic (or sandy) inclusions interspersed within a well-developed clay-rich argillic horizon (Bt) (Fig. 1) (Loomis 1989; Watts 1993). In addition, grove vegetation occurred almost entirely within areas where the argillic horizon was absent (Fig. 1). This suggests that there might be strong spatial associations between these coarse-textured non-argillic inclusions and grove vegetation in this region. However, it has been difficult to generalize this relationship to larger spatial scales based on spatially limited sampling. Even if this relationship that grove vegetation is present on non-argillic inclusions is true, it raises questions concerning cause and effect. Did the presence of grove vegetation disrupt the well-developed argillic horizon to form coarse-textured inclusions? For example, the modification of subsurface soil texture beneath woody patches as a result of below-ground faunal activity (e.g. termites) has been well-documented in other savanna ecosystems (Konaté

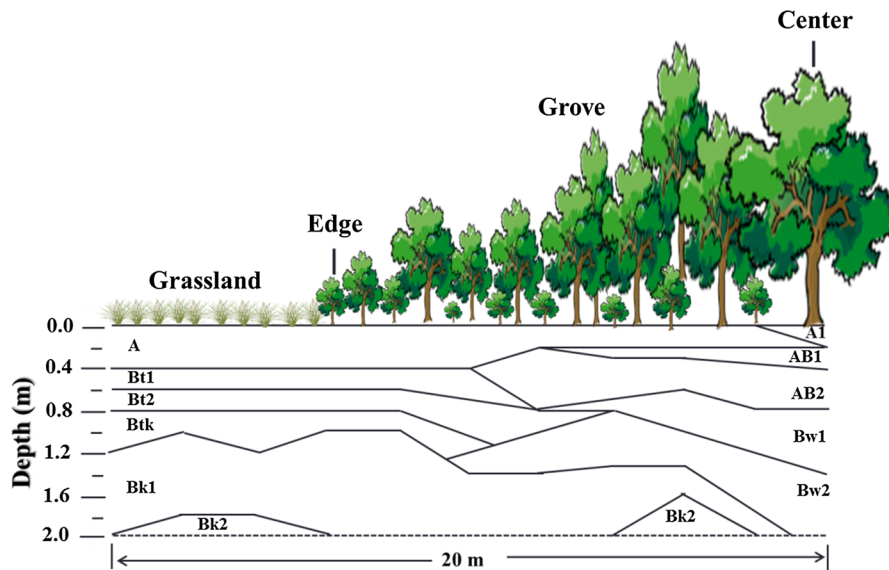


Fig. 1 Map of soil horizons to a depth of 2 m in a subtropical savanna ecosystem in southern Texas. The map was developed from a transect running from open grassland to the center of a

et al. 1999; Turner et al. 2006; Sileshi et al. 2010). Or, alternatively, did non-argillic inclusions form pedogenically (i.e., fluvial or aeolian depositional processes) before the current biota, favoring the establishment of grove vegetation and structuring the distribution of woody patches in this subtropical savanna?

The primary objective of this study was to quantify the landscape-scale distribution of soil texture throughout an entire soil profile to map the locations of non-argillic inclusions, and spatially associate them with the current distribution of grove vegetation. Specific objectives were to (1) map the locations of non-argillic inclusions across this landscape; (2) spatially associate non-argillic inclusions with the current distribution of grove vegetation to infer cause-effect relationships; and (3) assess the potential for new grove development and future landscape evolution. We hypothesize that spatial heterogeneity of subsurface soil texture drives the distribution of grove vegetation and structures the spatial pattern of woody patches in this subtropical savanna, rather than the alternative that current grove vegetation induced the discontinuous subsurface argillic horizon. If this is true, current grove vegetation should be located exclusively on non-argillic inclusions, but some non-argillic inclusions might not yet be colonized by grove

grove, and shows that the grove vegetation is largely confined to areas where the argillic horizon (B_t) is absent (based on data from Watts 1993). (Color figure online)

vegetation. These unoccupied non-argillic inclusions then have the potential to develop grove vegetation and shape the future landscape evolution. To test this hypothesis, we took 320 spatially georeferenced soil cores to a depth of 1.2 m across a 160 m × 100 m landscape and measured soil texture within multiple depth increments. These measurements enabled us to model the spatial structure of soil texture using variogram analysis, and to map the distribution of non-argillic inclusions across this landscape using spatial interpolation (i.e. ordinary kriging).

Materials and methods

Site description

This study was conducted at the Texas A&M AgriLife La Copita Research Area (27°40'N, 98°12'W), approximately 65 km west of Corpus Christi, Texas. Climate is subtropical, with a mean annual temperature of 22.4 °C and an average annual precipitation of 680 mm distributed mostly in May and September. Elevation ranges from 75 to 90 m above sea level. The landscape consists of fairly gentle slopes (1–3%), and is comprised of nearly level uplands, lower-lying drainage woodlands, and playas.

This study was confined to upland portions of the landscape. Upland soils are sandy loam (Typic and Pachic Argiustolls) (Boutton et al. 1998). The vegetation is characterized as subtropical savanna parkland, consisting of a continuous C_4 grassland matrix, with discrete woody patches interspersed within that matrix. Woody patches are categorized into smaller shrub clusters and large groves. Clusters, usually with diameters <10 m, are comprised of a single honey mesquite tree with up to 15 understory shrub/tree species. Groves, usually with diameters >10 m, are comprised of several clusters that have fused together (Archer 1995; Bai et al. 2012). Common understory shrub/tree species in clusters and groves include *Zanthoxylum fagara*, *Schaefferia cuneifolia*, *Celtis pallida*, *Zizyphus obtusifolia*, *Lycium berlandieri*, *Mahonia trifoliolata*, and *Opuntia leptocaulis*. Common grasses that dominate the C_4 grassland matrix include *Paspalum setaceum*, *Setaria geniculata*, *Bouteloua rigidisetata*, and *Chloris cucullata*. Additional details on vegetation can be found in Archer et al. (1988), Archer (1995) and Boutton et al. (1998).

Field sampling

A $160\text{ m} \times 100\text{ m}$ plot consisting of $10\text{ m} \times 10\text{ m}$ grid cells was established in 2002 on an upland portion of the study site (Fig. 2), which included all of the

upland landscape elements: grasslands, clusters and groves (Bai et al. 2009; Liu et al. 2011). Each corner of each $10\text{ m} \times 10\text{ m}$ grid cell was marked with a PVC pole and georeferenced using a GPS unit (Trimble Pathfinder Pro XRS, Trimble Navigation Limited, Sunnyvale, CA, USA) based on a UTM projection (WGS 1984).

Two points within each $10\text{ m} \times 10\text{ m}$ cell were randomly selected for sampling soil (320 points, Fig. 2) in July 2014. Landscape elements for each soil sampling point were categorized as grassland, cluster, or grove. Distances from each soil sampling point to two georeferenced cell corners were measured. At each soil sampling point, two adjacent soil cores (2.8 cm in diameter \times 120 cm in depth) were collected with a PN150 JMC Environmentalist's Subsoil Probe (Clements Associates Inc., Newton, IA, USA). Each soil core was subdivided into 6 depth increments (0–5, 5–15, 15–30, 30–50, 50–80, and 80–120 cm). One soil core was oven-dried (105 °C for 48 h) to determine soil bulk density. Depth increments from the other core were passed through a 2-mm sieve to remove large organic fragments, then dried at 60 °C for analysis of soil texture and other soil physico-chemical parameters. An additional adjacent soil core (10 cm in diameter \times 15 cm in depth) was collected to meet the mass requirement of soil texture analysis for 0–5 and 5–15 cm soil depth increments.

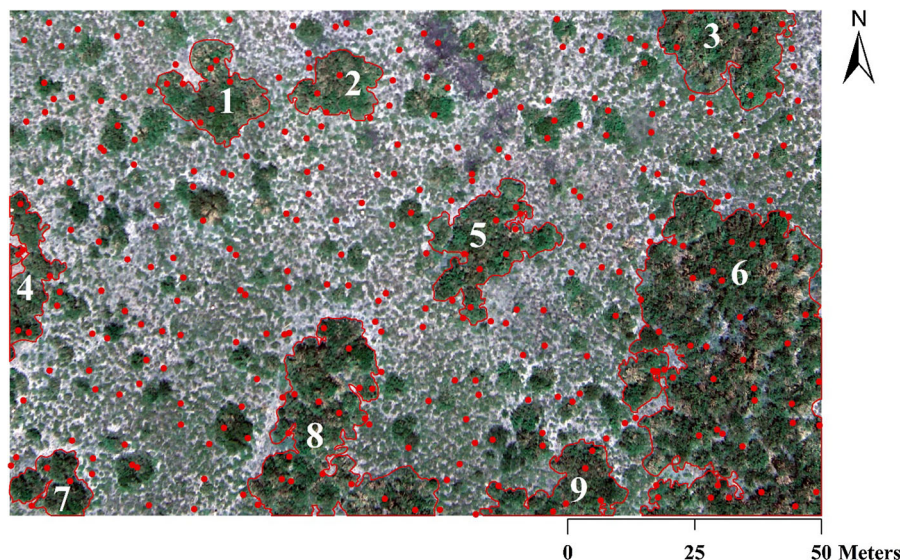


Fig. 2 Aerial photograph of the $160\text{ m} \times 100\text{ m}$ study area. Red dots indicate 320 random soil sampling points. Red lines indicate the edges of groves. (Color figure online)

A color infrared aerial photograph was acquired in July 2015. To facilitate georeferencing of the photo, 14 evenly distributed cell corners with 30 cm × 30 cm white surfaces fastened on the top of the PVC poles were used as ground control points.

Lab analyses

Soil texture was analyzed by the hydrometer method according to Sheldrick and Wang (1993). Briefly, 80.0 ± 1.0 g oven-dried soil was mixed with 2.0 g sodium hexametaphosphate, placed into a soil dispersing cup, and soaked with deionized water. The cup was then attached to a mixer for 10 min to disrupt soil aggregates. The soil suspension was transferred to a graduated cylinder and filled with deionized water to the 1000-ml mark. A calibrated hydrometer was placed carefully into the soil suspension after the suspension was well mixed with a plunger. After 40 s, the hydrometer reading was recorded, and this process was repeated to obtain an average. The hydrometer was removed from the soil suspension and temperature was recorded. After 2-h, hydrometer and temperature readings were repeated on each soil suspension. Sand, silt, and clay concentrations were calculated according to Sheldrick and Wang (1993).

Roots were separated from oven-dried soil samples after determining soil bulk density through washing with sieves, and sorted into fine roots (<2 mm in diameter) and coarse roots (>2 mm). All roots samples were then oven-dried (65 °C) to constant weight for biomass.

Statistical analyses

Mantel tests were used to test spatial autocorrelation of soil variables using PASSaGE 2 (Rosenberg and Anderson 2011). Significance (two-tailed) of Mantel tests was determined by permutation (1000 randomizations). Mixed model was used to compare soil variables in different landscape elements within each soil depth increment using JMP Pro 12 (SAS Institute Inc., Cary, NC, USA). Spatial autocorrelation of variable was considered as a spatial covariance component for adjustment in mixed model (Littell et al. 2006). *Post-hoc* comparisons of these variables in different landscape elements were conducted using the Tukey–Kramer method which adjusts for unequal sample sizes. Pearson correlation coefficients were determined between total fine root biomass to a depth of 1.2 m and soil sand, silt

and clay concentration for each soil layer using R statistical software (R Development Core Team 2011). A modified *t* test (Dutilleul et al. 1993) which accounts for the effects of spatial autocorrelation was used to determine the significance levels of these correlation coefficients. For all these statistical analyses, a cutoff of $p = 0.05$ was used to indicate significant differences.

Color-infrared aerial photography (6 cm × 6 cm in resolution) was processed and georeferenced using ERDAS Imagine 9.2 (ERDAS, Inc., Atlanta, GA, USA). Edges of woody patches (clusters and groves) were manually delineated using ArcGIS 10.1 (ESRI, Redlands, CA, USA). The centroid (X and Y coordinates) of each woody patch was calculated using Calculate Geometry in ArcGIS 10.1. Ordinary kriging was used in Spatial Analyst Tools of ArcGIS 10.1 for spatial interpolation of values at unsampled locations based on 320 random sampling points and their spatial structure determined by using variogram analysis (see supplementary materials for more details). Soil clay concentration contours (at 2% intervals) for the 80–120 cm soil layer were generated using Spatial Analyst Tools in ArcGIS 10.1.

The spatial pattern of clusters was examined with Ripley's *K*-function, a second-order statistic for quantifying spatial patterns (Ripley 1981), based on the calculated centroid of each cluster. The sample statistic $K(d)$ is calculated separately for a range of distance d , to examine the distribution pattern of clusters as a function of scale. A weighting approach was used to correct for edge effects (Haase 1995). For an easier interpretation, the result of the spatial pattern analysis was plotted as $\sqrt{K[(d)/\pi]} - d$ against d . The statistic $\sqrt{K[(d)/\pi]} - d$ was tested with 1000 randomizations at a 99% confidence interval. If the sample statistic stays within the confidence interval, the null hypothesis of complete spatial randomness is true, values above the confidence interval indicate aggregation, while values below the confidence interval indicate a regular or uniform distribution.

Results

Landscape-scale patterns of soil texture along the soil profile

Results of the Mantel test indicated that soil sand, silt, and clay concentrations for all examined soil layers

were spatially autocorrelated ($p < 0.05$, Table 1). Soil sand concentration decreased, while soil silt and clay concentrations increased with soil depth across this landscape (Table 2; Fig. 3). On average, soil sand concentration decreased 25.6% from the upper 0–5 cm soil layer to the lower 80–120 cm soil layer, while soil silt and clay concentrations increased 26.2 and 127.2%, respectively. Soil sand concentration beneath groves was comparable with that beneath grasslands for 0–5, 5–15, and 15–30 cm soil layers, but was significantly higher in the 50–80 and 80–120 cm soil layers (Table 2). No significant differences were found among landscape elements for soil clay concentration for the upper 0–30 cm soil layers, while soil clay concentration beneath groves was significantly lower than that beneath grasslands for the lower 30–120 cm soil layers (Table 2).

Ordinary kriging based on the data for 320 sampling points and variogram analysis provided an interpolation tool to estimate the values of unsampled locations, and to develop maps of soil sand, silt and clay concentrations across this landscape and along the soil profile (Fig. 3). Spatial distributions of soil sand, silt and clay concentrations for the upper 0–30 cm soil layers were directional across this landscape (Fig. 3). Soil sand concentration was higher in the northern portion of this landscape and decreased gradually toward the southeast corner (Fig. 3). In contrast, soil silt and clay concentrations were concentrated at the southeast corner and lower values were found in north and northwest directions (Fig. 3). For example, soil clay concentration in the 0–5 cm soil layer doubled from the north towards the southeast.

In addition, the spatial distribution of soil sand, silt and clay concentrations revealed the presence of non-argillic inclusions dispersed within a matrix of relatively higher clay concentration at depths >30 cm (Fig. 3). This spatial pattern was especially prominent within the 80–120 cm soil layer (Fig. 3), where the clay concentration at the center of these non-argillic inclusions was half less than the values in adjacent soil with a clayey argillic horizon. When aerial photography is compared visually to the kriged map of either soil clay or sand concentration at the 80–120 soil layers, it is obvious that all of the groves are located on these non-argillic inclusions.

Spatial correlations between fine root biomass and soil texture

Results of the Mantel test indicated that fine root biomass in soil layers above 50 cm was spatially autocorrelated ($p < 0.05$, Table 1). Total fine root biomass to a depth of 120 cm beneath woody patches (clusters: $2291 \pm 97.44 \text{ g m}^{-2}$, $n = 41$; groves: $2562.52 \pm 74.08 \text{ g m}^{-2}$, $n = 79$) was significantly higher than that for grassland ($1075.38 \pm 18.79 \text{ g m}^{-2}$, $n = 200$). This pattern was true for each individual soil depth increment along the profile (Table 2). Interestingly, fine root biomass beneath groves was significantly higher than that beneath clusters for the 50–80 and 80–120 cm soil layers (Table 2). A kriged map of total fine root biomass to a depth of 120 cm based on 320 random sampling points indicated that fine root biomass was highest at the center of woody patches (clusters and groves), decreased towards the canopy edges of woody patches

Table 1 Results of Mantel tests for spatial autocorrelations of soil sand, silt, clay concentration and fine root biomass along the soil profile

Soil layers (cm)	Sand		Silt		Clay		Fine root biomass	
	Mantel's r	<i>p</i>	Mantel's r	<i>p</i>	Mantel's r	<i>p</i>	Mantel's r	<i>p</i>
0–5	0.265	0.001	0.233	0.001	0.208	0.001	0.090	0.001
5–15	0.292	0.001	0.220	0.001	0.245	0.001	0.086	0.001
15–30	0.236	0.001	0.263	0.001	0.170	0.001	0.061	0.002
30–50	0.110	0.001	0.250	0.001	0.073	0.002	0.042	0.036
50–80	0.074	0.002	0.077	0.001	0.081	0.001	0.035	ns
80–120	0.071	0.003	0.052	0.038	0.088	0.001	0.038	ns

Significance (p , two tailed) of Mantel tests was determined by permutation (1000 randomizations), ns indicates not significant ($p > 0.05$)

Table 2 Mean and standard error (SE) of soil sand, silt, and clay concentrations, and fine root biomass in contrasting landscape elements along the soil profile in a subtropical savanna

	Soil layers (cm)					
	0–5	5–15	15–30	30–50	50–80	80–120
Sand (%)						
Grassland	76.42 (0.15)a	74.49 (0.15)a	71.50 (0.14)a	67.21 (0.20)b	62.85 (0.21)b	55.75 (0.33)b
Cluster	75.42 (0.43)a	74.13 (0.43)ab	71.39 (0.39)ab	67.80 (0.58)ab	62.99 (0.78)b	55.40 (0.86)b
Grove	74.99 (0.40)b	73.32 (0.43)b	70.44 (0.46)b	68.11 (0.50)a	64.90 (0.56)a	58.96 (0.86)a
Silt (%)						
Grassland	10.75 (0.07)b	10.13 (0.06)a	10.69 (0.06)a	11.11 (0.07)a	12.18 (0.07)a	14.12 (0.07)a
Cluster	11.11 (0.21)a	10.69 (0.17)a	11.10 (0.15)a	11.34 (0.15)a	12.15 (0.16)a	13.97 (0.18)a
Grove	11.78 (0.18)a	11.16 (0.16)a	11.65 (0.14)a	11.88 (0.14)a	12.20 (0.14)a	13.46 (0.16)b
Clay (%)						
Grassland	12.83 (0.11)a	15.38 (0.11)a	17.81 (0.11)a	21.68 (0.19)a	24.97 (0.18)a	30.12 (0.28)a
Cluster	13.46 (0.30)a	15.18 (0.31)a	17.51 (0.30)a	20.85 (0.55)b	24.86 (0.70)a	30.63 (0.71)a
Grove	13.23 (0.25)a	15.52 (0.30)a	17.91 (0.35)a	20.00 (0.40)c	22.89 (0.48)b	27.57 (0.73)b
Fine root biomass (g m⁻²)						
Grassland	173.69 (5.41)b	216.90 (5.81)b	208.31 (5.15)b	202.83 (4.77)b	154.86 (4.17)c	118.79 (4.72)c
Cluster	506.07 (34.66)a	535.91 (30.66)a	411.69 (24.29)a	353.10 (16.18)a	264.04 (18.13)b	221.03 (15.63)b
Grove	509.99 (22.04)a	573.78 (21.93)a	461.66 (16.62)a	381.62 (17.16)a	328.16 (13.64)a	307.31 (14.52)a

Different letters indicated significant different ($p < 0.05$) between means in landscape elements based on mixed models. Number of samples: grassland = 200, cluster = 41, grove = 79

and reached the lowest values within the grassland matrix (Fig. 4). The kriged map of total fine root biomass displayed a spatial pattern similar to that of vegetation cover, especially the distribution of grove vegetation (Figs. 2, 4). Thus, total fine root biomass was used as an indicator of vegetation cover to correlate with soil texture. Quantitatively, there were no significant correlations either between total fine root biomass and soil sand concentration or between total fine root biomass and soil clay concentration for soil layers above 30 cm (Table 3). However, below 30 cm where the non-argillic inclusions begin, total fine root biomass was significantly and positively correlated with soil sand concentration, while was significantly and negatively correlated with soil clay concentration (Table 3).

Spatial distribution of grove vegetation associated with subsurface soil texture

Based on the kriged map of soil clay concentration for the 80–120 cm soil layer, a contour map with 2% intervals was developed to reveal the locations of non-argillic inclusions which were labeled with capitalized

letters (Fig. 5). This depth was selected because it most clearly delineates the positions of the non-argillic inclusions. Categorized landscape elements were superimposed on the contour map to show the positions of groves in relation to non-argillic inclusions. Generally, each grove exclusively occupied one of these non-argillic inclusions, except grove no. 8 which occupied three coarse-textured inclusions (J, K and L), and may have coalesced from three individual groves (Table 4; Fig. 5). No grove was found beyond a non-argillic inclusion (Fig. 4). Non-argillic inclusions C and F are still not occupied by groves (Fig. 4). Exact positional correspondences, unoccupied non-argillic inclusions, and spatial correlations between total fine root biomass and soil texture mentioned above all support the hypothesis that spatial heterogeneity of subsurface soil texture drives the distribution of grove vegetation. It appears unlikely that groves modified subsurface soil to form these non-argillic inclusions. If the hypothesis holds true, it implies that non-argillic inclusions favor the formation of grove vegetation, and the future expansion of grove vegetation may be predictable (Table 4). Groves no. 1, 2, 3, 4, 5, and 7 only occupied portions

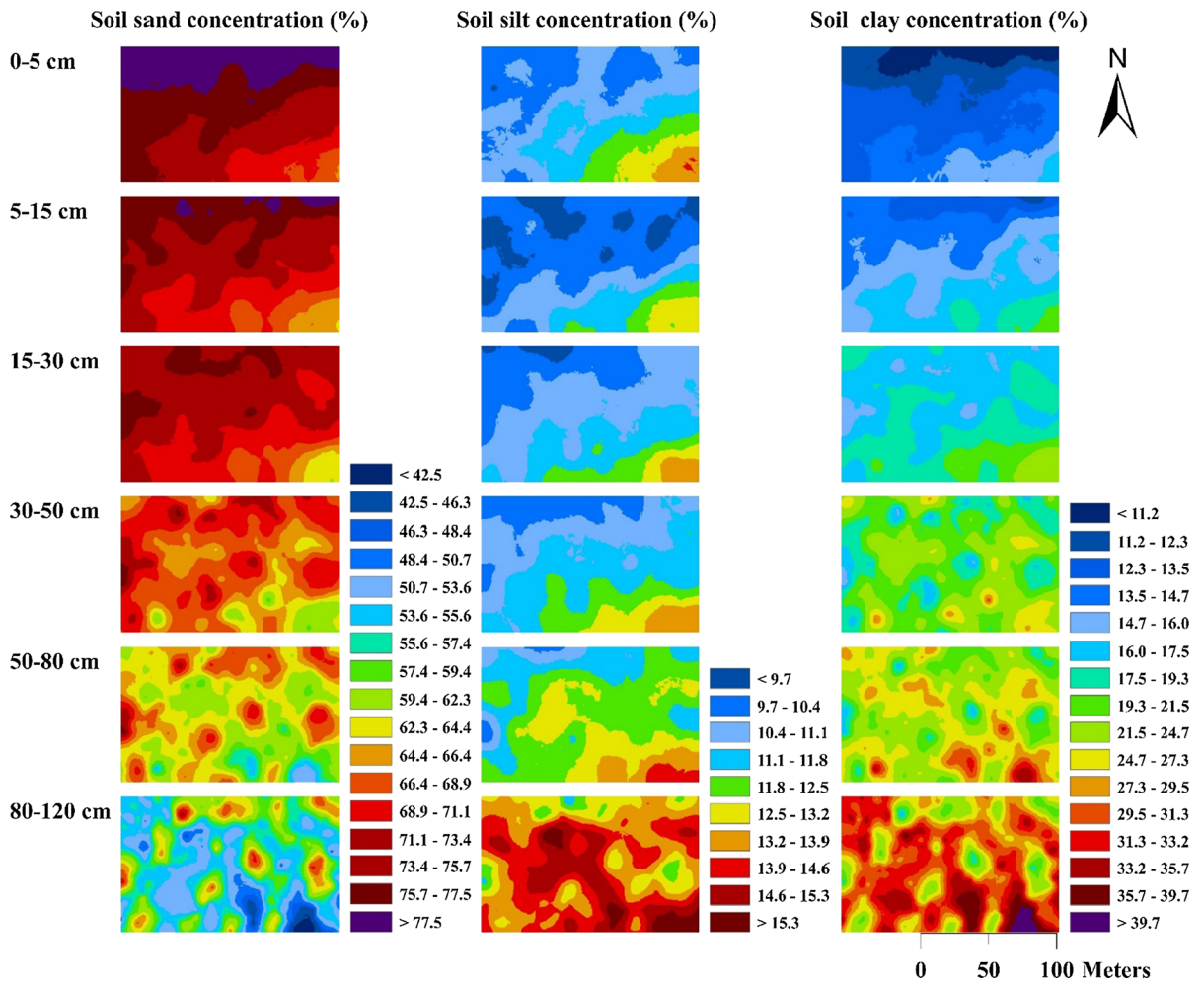


Fig. 3 Kriged maps of soil sand, silt and clay concentrations along the soil profile based on 320 random sampling points across this landscape in a subtropical savanna. (Color figure online)

Fig. 4 Kriged map of total fine root biomass (kg m^{-2}) to a depth of 120 cm based on 320 random sampling points across this landscape in a subtropical savanna. (Color figure online)

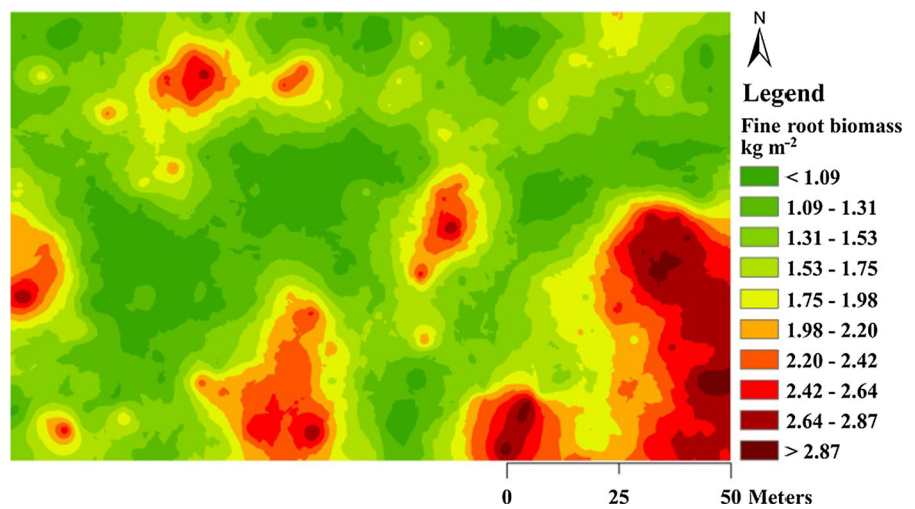


Table 3 Pearson correlation coefficients (r) for the relationships between total fine root biomass, soil clay, silt, and sand concentrations along the soil profile

Depth (cm)	Total fine root biomass					
	Sand		Silt		Clay	
	r	p	r	p	r	p
0–5	−0.181	ns	0.245	0.022	0.098	ns
5–15	−0.111	ns	0.315	0.004	−0.026	ns
15–30	−0.068	ns	0.283	0.011	−0.049	ns
30–50	0.180	0.046	0.201	ns	−0.271	<0.0001
50–80	0.239	0.005	−0.032	ns	−0.266	<0.0001
80–120	0.228	0.004	−0.243	0.002	−0.210	0.008

Statistical significance (p) of correlation coefficients was calculated based on a modified t test (Dutilleul et al. 1993) which takes the effect of spatial autocorrelation into account within data sets; ns indicates not significant ($p > 0.05$)

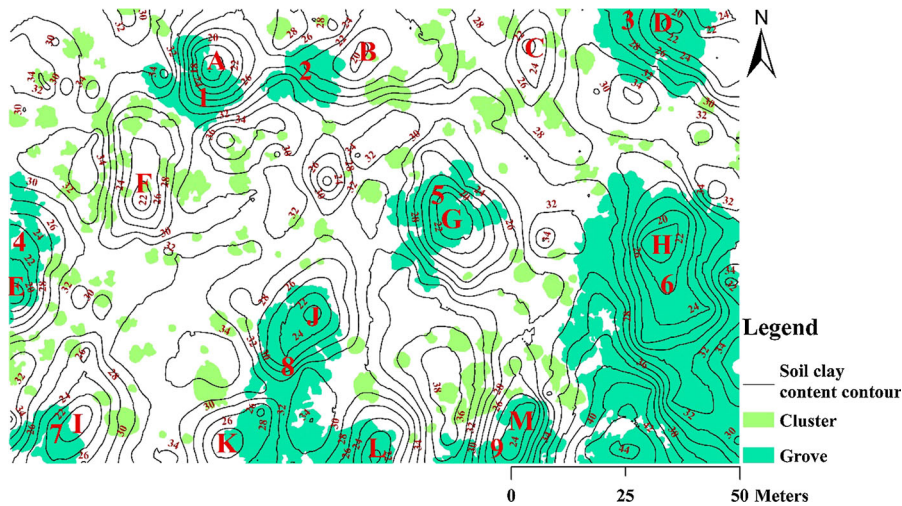


Fig. 5 Soil clay concentration contours (at 2% intervals) for the 80–120 cm soil layer superimposed on the categorized landscape elements for this 160 m × 100 m landscape in a

subtropical savanna. Capital letters indicate locations of non-argillic inclusions. (Color figure online)

of non-argillic inclusions, and may eventually expand to fill unoccupied portions of these inclusions. Non-argillic inclusions C and F have the potential to form grove vegetation in the future (Fig. 5).

Conceptual model of landscape evolution

Second order point pattern analysis showed that the spatial distribution of clusters was random at most detected scales, with marginally aggregated patterns at certain scales (Fig. 6). This marginal aggregation might be ascribed to the exclusion of groves when performing the analysis. If each grove was considered to be formed from one cluster, the spatial pattern of

clusters was completely random (Fig. S2). Based on the random distribution of clusters and the spatial association between grove vegetation and non-argillic inclusions, a conceptual model of landscape evolution is proposed (Fig. 7). Woody plants, mainly honey mesquite, encroached into grasslands that was once exclusively dominated by C_4 grasses, serving as nurse plants for other woody plants and initiating a process of autogenic succession to form clusters (Fig. 7) (Archer et al. 1988). This phase of cluster formation was a completely random and ongoing process. If clusters coincidentally occupied pre-existing non-argillic inclusions, they eventually expanded and coalesced with adjacent clusters that occupied the

Table 4 The status of non-argillic inclusions occupied by groves, and the potential expanding direction of groves

Sandy inclusions	Corresponding groves	Status occupied by groves	Potential expanding direction
A	1	Partially	Northeast; May coalesce with grove no. 2
B	2	Partially	Northeast; May coalesce with grove no. 1 and other three adjacent large clusters
D	3	Partially	Southeast
E	4	Partially	East or Southeast; May coalesce with several adjacent clusters
G	5	Partially	Southeast
H	6	Completely	Slowly all directions; May coalesce with grove no. 9
I	7	Partially	Northeast
K, J, L	8	Extensively	Slowly all directions
M	9	Extensively	Slowly all directions; may coalesce with several adjacent clusters or grove no. 6
C, F	NA	Not occupied	Have the potential to form groves

Potential expanding direction is developed based on the hypothesis that non-argillic inclusions are susceptible to the establishment/expansion of grove vegetation

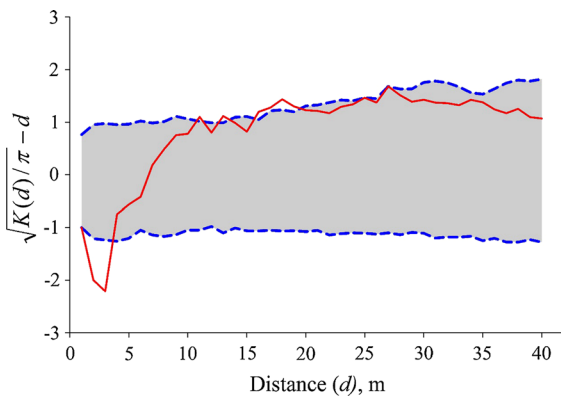


Fig. 6 Plot of the sample statistic $\sqrt{K(d)/\pi} - d$ against distance d reveals the spatial pattern of clusters at various scales. The sample statistic was tested based on 1000 randomizations of actual data. Dotted lines show 99% confidence intervals. Values staying within the confidence intervals indicate complete spatial randomness; values above confidence intervals indicate aggregation, while values below signify regularity

same inclusion to form groves, and became prominent and persistent features of the landscape (Fig. 7). Clusters developing where the argillic horizon was present would ultimately undergo a process of self-thinning and senescence, or become stable landscape elements (Fig. 7). Groves, together with stable clusters, developed within the grassland matrix to form the current landscape (Fig. 7). This phase of landscape development was structured by the spatial heterogeneity of subsurface soil texture.

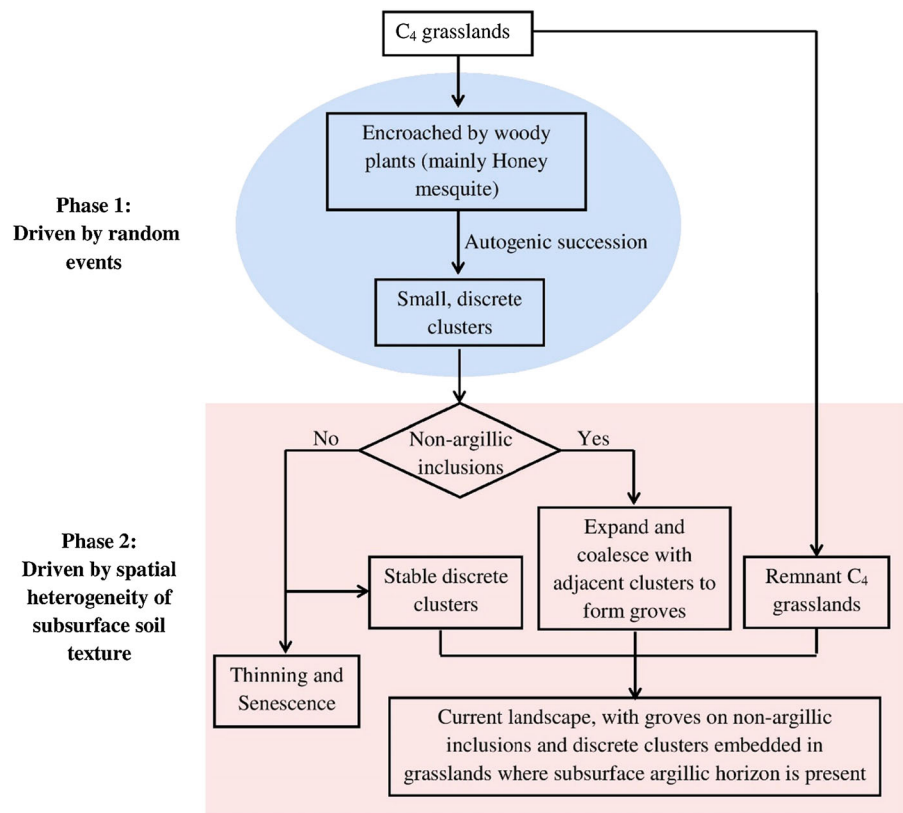
Discussion

Landscape-scale spatial patterns of soil texture along the soil profile

Spatial patterns of soil texture in the upper 30 cm of the soil profile were directional, with sand concentration decreasing and silt and clay concentrations increasing from the north towards the southeastern corner of this landscape (Fig. 3). These spatial patterns were consistent with a previous study in the same plot in which soil texture in the upper 15 cm soil layer was examined (Bai et al. 2009). The anisotropic distribution of soil texture in the upper portion of the soil profile is likely related to landscape processes that are influenced by elevation, such as runoff and erosion.

Patches that lacked an argillic horizon and had a higher sand concentration were interspersed in a laterally extensive subsurface argillic horizon, particular at depths >50 cm (Fig. 3). The spatial association between grove vegetation and these non-argillic inclusions presented in this study (Fig. 5) raised an additional cause-effect question. Did grove vegetation contribute to the formation of non-argillic inclusions? Since the modification of subsurface soil texture by woody plant associated below-ground faunal activities has been reported in other savanna ecosystems (Lobry de Bruyn and Conacher 1990; Konaté et al. 1999;

Fig. 7 A conceptual model of landscape evolution in an upland subtropical savanna ecosystem in southern Texas, USA



Turner et al. 2006), it's reasonable to hypothesize that extensively observed rodent (pack rat, *Neotoma micropus*) and leaf-cutter ant (*Atta texensis*) burrowing and excavating activities confined to grove vegetation in this study area (Loomis 1989; Archer 1995; Liu et al. 2011) could have the potential to disrupt and obliterate a once continuous argillic soil horizon to form these non-argillic inclusions. If this assumption is correct, (1) soil clay concentration beneath grove vegetation in the upper soil layers should be significantly higher than non-grove soils due to faunal uplift-translocating activities, and (2) total clay concentration, when summed across the soil profile, should be comparable between grove and non-grove soils. However, no significant differences were detected in soil clay concentration between grove and non-grove soils in the upper 30 cm of soils (Table 2). Furthermore, soil cores at the center of groves were coarse-textured throughout the entire profile, and total clay concentration to a depth of 1.2 meters was significantly lower than in soil cores beyond grove boundaries (data not shown). These lines of evidence suggest the hypothesis that grove

vegetation is responsible for the formation of non-argillic inclusions is not tenable.

Alternatively, non-argillic inclusions are pre-existing and intrinsic features of this landscape. If this is true, there should be non-argillic inclusions which, by chance, have not yet been occupied by grove vegetation. In fact, across this landscape, two such inclusions have been mapped (labelled as C and F, Fig. 5), and stable carbon isotopic analysis excluded the possibility that these two inclusions have ever been occupied by C_3 woody plants (unpublished data). Therefore, it seems likely that the spatial heterogeneity of subsurface soil texture was generated pedogenically (i.e. fluvial or eolian depositional processes, Loomis 1989) prior to the recent vegetation changes that have transformed this landscape.

Spatial heterogeneity of subsurface soil texture drives the distribution of grove vegetation

Previous results from space-for time substitution models (Archer 1995), modelling studies of vegetation structure (Stokes 1999) and spatial patterns of soil

$\delta^{13}\text{C}$ (Bai et al. 2012) indicated that as new clusters were initiated by the encroachment of honey mesquite trees and existing clusters expanded, coalescence would occur to form groves where the argillic horizon was absent. Although the role of the non-argillic inclusions in grove formation has been recognized and documented (Loomis 1989; Watts 1993; Archer 1995), the distribution and abundance of these non-argillic inclusions has not been quantified at the landscape scale.

The landscape-scale 3-dimensional distribution of soil texture developed in this study provides additional direct evidence for the essential role that pre-existing non-argillic inclusions play in regulating the distribution of grove vegetation. In this study, we found that groves occurred only within non-argillic inclusions (Fig. 5). Based on the results of this study and previous findings (Archer et al. 1988; Loomis 1989; Watts 1993; Archer 1995; Stokes 1999; Bai et al. 2012), we present a conceptual model that recognizes the spatial heterogeneity of subsurface soil texture as a factor in vegetation change at the landscape scale (Fig. 7). The spatial distribution of existing clusters across this landscape was random, suggesting that the formation of clusters is entirely determined by the dispersion of honey mesquite seeds via animals, and their germination and establishment can occur on a wide range of soil conditions across this landscape, regardless of the subtle spatial heterogeneity of subsurface soil texture. However, clusters that coincidentally developed on non-argillic inclusions likely experienced more favorable growth conditions on these coarse-textured soils, and expanded laterally and ultimately fused with other clusters to form groves. In this study, we found that fine root biomass of woody plants beneath groves was significantly higher than beneath clusters in the 50–80 and 80–120 cm depth increments (Table 2), and total fine root biomass was significantly and positively correlated with soil sand concentration in the 30–50, 50–80, and 80–120 cm depth increments (Table 3). This suggests that coarse-textured subsoils may benefit the growth of woody plants by enabling root penetration deeper into the profile, providing them greater access to water and nutrients that are less accessible on those portions of the landscape where the argillic horizon is present. As woody plant communities develop within the non-argillic inclusions, they may also trigger a positive feedback loop by increasing soil nutrient pool sizes and turnover

rates (i.e. islands of fertility), which could further stimulate growth, recruitment, and survival of woody species (Schlesinger et al. 1996; Scholes and Archer 1997; Boutton et al. 1999; McCulley et al. 2004). In fact, honey mesquite trees on non-argillic inclusions were larger and older than their counterparts growing on subsoils with an argillic horizon (Archer 1995; Boutton et al. 1998), and total tree and shrub basal areas were 2.5 times more in groves than in clusters (Liu et al. 2010), reflecting enhanced woody plant growth and production on coarse-textured subsoils. In contrast, clusters that occur on soils with an argillic horizon are constrained in their expansion rates (Fig. 5). In this study, 121 clusters were observed, with an average size of 13.4 m², and 80% of them are less than 20 m². This may suggest that clusters, compared to groves, are unable to expand beyond a certain size across this landscape. As such, the current landscape is comprised of groves on non-argillic inclusions as large and relatively long-lived features, and comparatively transient and size-constrained clusters dispersed among the remnant C₄ grasslands where the argillic horizon is present (Fig. 7).

Although spatial heterogeneity of subsurface soil texture appears to function as a key determinant for the distribution of grove vegetation across this landscape, other factors, including plant–soil interactions and topography, should be considered in the expansion of grove vegetation. Once groves extensively or even completely occupy these easily colonized non-argillic inclusions and encounter resistance from the argillic soils that surround them, their expansion rates may be reduced. However, these groves may continue to play an active role in recruitment of woody plants around their canopy edges (even where the argillic horizon is present) by altering surficial soils and microclimate in ways that enhance the survival probability of these woody recruits. Areas at (or even beyond) canopy edges of groves may experience some degree of soil nutrient enrichment through leaf litter deposition, horizontal root extension (Watts 1993; Boutton et al. 2009; Bai et al. 2012), and/or potential transfer of N fixed by honey mesquite (Soper et al. 2015; Zhang et al. 2016). In addition, improved water regimes through water uptake and redistribution (Zou et al. 2005; Miller et al. 2010), and reduced light levels and temperature extremes (Archer 1995; Scholes and Archer 1997) likely characterize the edges of groves. These environmental modifications near grove edges

may collectively override the limitations of the argillic horizon and facilitate the recruitment of woody plants. An example of such a case is grove no. 8. Apparently, grove no. 8 coalesced from three individual groves that once occupied each of these non-argillic inclusions (J, K, and L), and expanded beyond these inclusions (Figs. 2, 5).

Implications for future landscape evolution

Mapped non-argillic inclusions across this landscape and the fact that subsurface coarse-textured soils favor the development of grove vegetation may provide a glimpse of future landscape evolution. Some of the current groves occupy only a portion of the non-argillic inclusions on which they occur, and therefore have the potential to expand into unoccupied portions of these inclusions. As these groves expand, they have the potential to coalesce with adjacent groves or stable clusters (Table 4). For example, grove 2 and three adjacent large clusters will likely expand towards the center of the sandy inclusion B, and coalesce to form an even larger grove (Fig. 5). Groves 1 and 2 are both actively expanding towards the northeast to colonize the remainder of their sandy inclusions, and will likely coalesce (Fig. 5). This prediction is consistent with a previous study in which spatial patterns of soil $\delta^{13}\text{C}$ and chronosequences of aerial photographs were used to infer vegetation dynamics in the same plot (Bai et al. 2009). Several large clusters have been established around unoccupied non-argillic inclusions C and F (Fig. 5); with time, they may expand and eventually coalesce to form grove vegetation. Groves that have extensively or even completely occupied entire non-argillic inclusions are still active in expansion due to the positive feedbacks from plant–soil interactions as mentioned above. However, more accurate predictions of the future rate and direction of grove expansion for this landscape will require detailed information about the subsurface soil texture–rainfall–topography relationships and plant–soil interactions (Wu and Archer 2005).

Based on forward simulation using transition probabilities, Archer (1995) concluded that the present vegetation configuration in this subtropical savanna is an intermediate stage in the conversion of grassland to closed-canopy woodland, and this conversion will be completed within the next 180 years. Our study also

suggests that the present landscape still has the capacity for further woody plant expansion. Without major disturbances (i.e. fire, drought, and insect outbreak), current coverage of grove vegetation (27.3%) may be doubled through the expansion of existing groves and the formation of new groves on unoccupied portions of these non-argillic inclusions. Furthermore, based on historical aerial photographs, cluster coverage for this study plot increased from 4.3% in 1930 to current coverage of 10.3%, indicating that cluster formation is an ongoing process. Taken together, these patterns suggest the present landscape is likely to evolve to a closed-canopy woodland configuration in the future.

Conclusion

In savanna ecosystems, vegetation patchiness is a key regulator of ecosystem functions and services. However, the mechanisms responsible for the distribution of woody patches in savanna landscapes remain unclear. In this study, landscape-scale kriged maps of soil texture derived from spatially-specific soil samples taken to a depth of 1.2 m allowed us to reveal the spatial heterogeneity in subsurface soil texture (particularly the presence and location of non-argillic inclusions) as an intrinsic feature of this landscape. Exact positional correspondences between mapped non-argillic inclusions and the distribution of grove vegetation, and spatially correlated relationships between total fine root biomass and soil texture, collectively suggest that the spatial heterogeneity in subsurface soil texture functioned as a dominant factor driving the formation and distribution of grove vegetation. Based on inferences from previous studies and this study, a conceptual model was proposed to explain the evolution of current landscape. The establishment of clusters is a random ongoing process which largely depends on the seedling recruitment of woody plants, while the formation of groves appears to be strongly regulated by the spatial heterogeneity of subsurface soil texture. Since coarse-textured non-argillic inclusions enable the formation of grove vegetation, future landscape development is predicted based on kriged maps of soil texture. Without major disturbances, current woody cover may double as these mapped non-argillic inclusions are completely occupied by grove vegetation, and this landscape may

have the potential to develop into canopy-closed woodlands in the future. We suggest that spatial heterogeneity of subsurface soil properties (i.e. soil texture, water regimes, and nutrient status) should be considered in the study of savanna ecology since these heterogeneities could shape the spatial patterns of woody vegetation which strongly determine savanna ecosystem services and function.

Acknowledgements Yong Zhou was supported by the Sid Kyle Graduate Merit Assistantship from Department of Ecosystem Science and Management, Texas A&M University. We thank two anonymous reviewers for helpful comments that improved the manuscript. We thank also David McKown, manager of the La Copita Research Area, for assistance with on-site logistics, and Dr. Ayumi Hyodo and Ryan Mushinski for assistance with lab work. This research was supported by an NSF Doctoral Dissertation Improvement Grant (DEB/DDIG-1600790), the Howard McCarley Student Research Award from the Southwestern Association of Naturalist, an Exploration Fund Grant from the Explorers Club, and by USDA/NIFA Hatch Project (1003961).

References

- Anadón JD, Sala OE, Turner BL, Bennett EM (2014) Effect of woody-plant encroachment on livestock production in North and South America. *Proc Natl Acad Sci USA* 111:12948–12953
- Archer S (1995) Tree-grass dynamics in a *Prosopis*-thornscrub savanna parkland: reconstructing the past and predicting the future. *Ecoscience* 2:83–99
- Archer S, Scifres C, Bassham CR, Maggio R (1988) Autogenic succession in a subtropical savanna: conversion of grassland to thorn woodland. *Ecol Monogr* 58:111–127
- Archer SR, Boutton TW, Hibbard K (2001) Trees in grasslands: biogeochemical consequences of woody plant expansion. In: Schulze E-D, Harrison SP, Heimann M, Holland EA, Lloyd J, Prentice IC, Schimel D (eds) *Global biogeochemical cycles in the climate system*. Academic Press, San Diego, pp 115–137
- Arshad MA (1982) Influence of the termite *Macrotermes michaelseni* (Sjöst) on soil fertility and vegetation in a semi-arid savannah ecosystem. *Agro-ecosystems* 8:47–58
- Bai E, Boutton TW, Liu F, Wu XB, Archer SR (2012) Spatial patterns of soil $\delta^{13}\text{C}$ reveal grassland-to-woodland successional processes. *Org Geochem* 42:1512–1518
- Bai E, Boutton TW, Wu XB, Liu F, Archer SR (2009) Landscape-scale vegetation dynamics inferred from spatial patterns of soil $\delta^{13}\text{C}$ in a subtropical savanna parkland. *J Geophys Res*. doi:10.1029/2008JG000839
- Bonachela JA, Pringle RM, Sheffer E, Coverdale TC, Guyton JA, Caylor KK, Levin SA, Tarnita CE (2015) Termite mounds can increase the robustness of dryland ecosystems to climatic change. *Science* 347:651–655
- Boutton TW, Archer SR, Midwood AJ (1999) Stable isotopes in ecosystem science: structure, function and dynamics of a subtropical savanna. *Rapid Commun Mass Spectrom* 13:1263–1277
- Boutton TW, Archer SR, Midwood AJ, Zitzer SF, Bol R (1998) $\delta^{13}\text{C}$ values of soil organic carbon and their use in documenting vegetation change in a subtropical savanna ecosystem. *Geoderma* 82:5–41
- Boutton TW, Liao JD, Filley TR, Archer SR (2009) Below-ground carbon storage and dynamics accompanying woody plant encroachment in a subtropical savanna. In: Lal R, Follett R (eds) *Soil carbon sequestration and the greenhouse effect*, vol 2. Soil Science Society of America, Madison, pp 181–205
- Brown JR, Archer S (1990) Water relations of a perennial grass and seedling vs adult woody plants in a subtropical savanna, Texas. *Oikos* 57:366–374
- Buitenwerf R, Bond WJ, Stevens N, Trollope WSW (2012) Increased tree densities in South African savannas: >50 years of data suggests CO_2 as a driver. *Global Change Biol* 18:675–684
- Dutilleul P, Clifford P, Richardson S, Hemon D (1993) Modifying the t test for assessing the correlation between two spatial processes. *Biometrics* 49:305–314
- Haase P (1995) Spatial pattern analysis in ecology based on Ripley's K-function: introduction and methods of edge correction. *J Veg Sci* 6:575–582
- Hamerlynck EP, McAuliffe JR, Smith SD (2000) Effects of surface and sub-surface soil horizons on the seasonal performance of *Larrea tridentata* (creosotebush). *Funct Ecol* 14:596–606
- Higgins SI, Bond WJ, Trollope WS (2000) Fire, resprouting and variability: a recipe for grass–tree coexistence in savanna. *J Ecol* 88:213–229
- Konaté S, Le Roux X, Tessier D, Lepage M (1999) Influence of large termitaria on soil characteristics, soil water regime, and tree leaf shedding pattern in a West African savanna. *Plant Soil* 206:47–60
- Littell RC, Milliken GA, Stroup WW, Wolfinger RD, Schabenberger O (2006) SAS for mixed models. SAS Institute Inc., Cary, NC, USA
- Liu F, Wu X, Bai E, Boutton TW, Archer SR (2010) Spatial scaling of ecosystem C and N in a subtropical savanna landscape. *Global Change Biol* 16:2213–2223
- Liu F, Wu X, Bai E, Boutton TW, Archer SR (2011) Quantifying soil organic carbon in complex landscapes: an example of grassland undergoing encroachment of woody plants. *Global Change Biol* 17:1119–1129
- Lobry de Bruyn LA, Conacher AJ (1990) The role of termites and ants in soil modification—a review. *Soil Res* 28:55–93
- Loomis LE (1989) Influence of heterogeneous subsoil development on vegetation patterns in a subtropical savanna parkland, Texas. Dissertation, Texas A&M University
- McAuliffe JR (1994) Landscape evolution, soil formation, and ecological patterns and processes in Sonoran Desert bajadas. *Ecol Monogr* 64:111–148
- McCulley RL, Archer SR, Boutton TW, Hons FM, Zuberer DA (2004) Soil respiration and nutrient cycling in wooded communities developing in grassland. *Ecology* 85:2804–2817
- Miller GR, Chen X, Rubin Y, Ma S, Baldocchi DD (2010) Groundwater uptake by woody vegetation in a semiarid oak savanna. *Water Resour Res* 46:W10503

- Pringle RM, Doak DF, Brody AK, Jocqué R, Palmer TM (2010) Spatial pattern enhances ecosystem functioning in an African savanna. *PLoS Biol* 8:e1000377
- R Development Core Team (2011) R: a language and environment for statistical computing. R Foundation for Statistical Computing, Vienna
- Ratajczak Z, Nippert JB, Collins SL (2012) Woody encroachment decreases diversity across North American grasslands and savannas. *Ecology* 93:697–703
- Ripley BD (1981) *Spatial statistics*. Wiley, Hoboken
- Rosenberg MS, Anderson CD (2011) PASSaGE: pattern analysis, spatial statistics and geographic exegesis Version 2. *Methods Ecol Evol* 2:229–232
- Sankaran M, Ratnam J, Hanan NP (2004) Tree–grass coexistence in savannas revisited—insights from an examination of assumptions and mechanisms invoked in existing models. *Ecol Lett* 7:480–490
- Sankaran M, Hanan NP, Scholes RJ, Ratnam J, Augustine DJ, Cade BS, Gignoux J, Higgins SI, Roux XL, Ludwig F, Ardo J, Banyikwa F, Bronn A, Bucini G, Caylor KK, Coughenour MB, Diouf A, Ekaya W, Fedral CJ, February EC, Frost PGH, Hiernaux P, Hrabar H, Metzger KL, Prins HHT, Ringrose S, Sea W, Tews J, Worden J, Zambatis N (2005) Determinants of woody cover in African savannas. *Nature* 438:846–849
- Sankaran M, Augustine DJ, Ratnam J (2013) Native ungulates of diverse body sizes collectively regulate long-term woody plant demography and structure of a semi-arid savanna. *J Ecol* 101:1389–1399
- Scheiter S, Higgins SI, Beringer J, Hutley LB (2015) Climate change and long-term fire management impacts on Australian savannas. *New Phytol* 205:1211–1226
- Schenk HJ, Jackson RB (2005) Mapping the global distribution of deep roots in relation to climate and soil characteristics. *Geoderma* 126:129–140
- Schlesinger WH, Raikes JA, Hartley AE, Cross AF (1996) On the spatial pattern of soil nutrients in desert ecosystems. *Ecology* 77:364–374
- Scholes RJ, Archer SR (1997) Tree-grass interactions in savannas. *Annu Rev Ecol Evol Syst* 28:517–544
- Sheldrick BH, Wang C (1993) Particle size distribution. In: Carter MR (ed) *Soil sampling and methods of analysis*. Canadian Society of Soil Science, Lewis Publishers, Ann Arbor, pp 499–511
- Sileshi GW, Arshad MA, Konaté S, Nkunika PO (2010) Termite-induced heterogeneity in African savanna vegetation: mechanisms and patterns. *J Veg Sci* 21:923–937
- Soper FM, Boutton TW, Sparks JP (2015) Investigating patterns of symbiotic nitrogen fixation during vegetation change from grassland to woodland using fine scale $\delta^{15}\text{N}$ measurements. *Plant Cell Environ* 38:89–100
- Stokes CJ (1999) *Woody plant dynamics in a south Texas savanna: pattern and process*. Dissertation, Texas A&M University
- Turner JS, Marais E, Vinte M, Mudengi A, Park WL (2006) Termites, water and soils. *Agricola* 16:40–45
- Van Auken OW (2000) Shrub invasions of North American semiarid grasslands. *Annu Rev Ecol Evol Syst* 31:197–215
- Volder A, Briske DD, Tjoelker MG (2013) Climate warming and precipitation redistribution modify tree–grass interactions and tree species establishment in a warm-temperate savanna. *Global Change Biol* 19:843–857
- Watts SE (1993) *Rooting patterns of co-occurring woody plants on contrasting soils in a subtropical savanna*. Thesis, Texas A&M University
- Wu XB, Archer SR (2005) Scale-dependent influence of topography-based hydrologic features on patterns of woody plant encroachment in savanna landscapes. *Landscape Ecol* 20:733–742
- Zhang HY, Yu Q, Lü XT, Trumbore SE, Yang JJ, Han XG (2016) Impacts of leguminous shrub encroachment on neighboring grasses include transfer of fixed nitrogen. *Oecologia* 180:1213–1222
- Zou CB, Barnes PW, Archer S, McMurtry CR (2005) Soil moisture redistribution as a mechanism of facilitation in savanna tree–shrub clusters. *Oecologia* 145:32–40